2012 IEEE International Conference on Control Applications (CCA)
Part of 2012 IEEE Multi-Conference on Systems and Control
October 3-5, 2012. Dubrovnik, Croatia

Digital Locking of a Three-Mirror Ring Cavity

Abhijit G. Kallapur, Dirk Schütte, Ian R. Petersen, Toby K. Boyson,
Elanor Huntington, S. Z. Sayed Hassen, Hongbin Song, Michèle Heurs

Abstract— **This paper presents results for digitally locking an experimental optical cavity. Locking an optical cavity refers to the process of matching the resonant frequency of the cavity with the input laser frequency in order to facilitate maximum energy build-up inside the cavity. The cavity used in this paper is a three-mirror ring cavity with a piezo actuator mounted on one of the mirrors, which is digitally controlled to hold the cavity in lock. An integral LQG controller is designed and digitally implemented in order to achieve cavity lock and the closed-loop step response is presented. This is compared with the closed-loop step response using a digital proportional-integral controller for the three-mirror cavity.**

I. INTRODUCTION

Optical cavities have been well researched in the literature due to their potential applications to the field of quantum optics. Indeed, optical feedback has played a major role in stabilizing these cavities for applications such as frequency stabilization of semiconductor lasers [1], cavity-enhanced spectroscopic techniques [2], [3], [4], cavity quantum electrodynamics [5], microcavities [6], [7], as well as in general atomic, molecular, and optical physics [8]. In the case where the optical cavity is injected with a continuous-wave laser source, it is required to lock the cavity to the frequency of the input laser in order to build maximum energy inside the cavity. Here, *locking* the cavity refers to matching the resonant frequency of the cavity with the input laser frequency. Any deviation between these frequencies is characterized in terms of the *detuning parameter* Δ and is an undesired effect. Though cavity locking can be achieved in many ways, one possible approach would be to vary the distance between the mirrors of the cavity, effectively varying the resonant frequency of the cavity to match the frequency of the input laser. From an experimental point of view, this method of frequency locking can be implemented by controlling a piezo-electic transducer (PZT) mounted on one of the mirrors. In the literature, the most common control mechanism used to lock optical cavities involves an analog proportional-integral (PI) controller which is tuned using a trial-and-error approach.

This work was supported by the Australian Research Council

A. Kallapur, I.Petersen, T.Boyson, E. Huntington, S. Sayed Hassen, and H. Song are with the School of Engineering and Information Technology, University of New South Wales at the Australian Defence Force Academy, Canberra ACT 2600, Australia. a.kallapur@adfa.edu.au, i.petersen@adfa.edu.au, t.boyson@adfa.edu.au, e.huntington@adfa.edu.au, h.song@adfa.edu.au, sayed.hassen@gmail.com

D. Schütte and M. Heurs are with the Centre for Quantum Engineering and Space-Time Research, Leibniz Universität, Hannover 30167, Germany. dirk.schuette@aei.mpg.de, michele.heurs@aei.mpg.de

The introduction of modern control techniques to experimental quantum optics was presented in [9], [10]. Here, a linear quadratic Gaussian (LQG) controller synthesis was discussed using a quadrature model for the optical cavity. Indeed, the advantages of using modern control techniques such as an LQG controller for locking optical cavities offer a systematic approach to controller design. Building on these ideas, Sayed Hassen et. al. implemented an integral LQG control scheme to lock a two-mirror optical cavity in [11], [12]. Here, the controller was designed by considering a state space model for the cavity-actuator system obtained using subspace system identification methods. The LQG controller was augmented with an integrator stage in order to eliminate slowly varying drift and offset errors.

In this paper, we consider the problem of digitally locking a three-mirror ring cavity using a proportional-integral (PI) controller as well as an integral LQG controller. We compare the performance of both controllers in terms of their closed-loop step response. A simple third-order model is obtained for the cavity using system identification methods, leading to a fourth-order model for the integral LQG controller. This is in contrast to the results presented in [11], [12] where a 13^{th}-order model is used for the plant, leading to a 15^{th}-order controller. This is further reduced to a sixth-order controller using model reduction techniques for the purpose of implementation.

The frequency response data for the plant is recorded using a digital signal analyzer and an equivalent state space model is obtained using the *System Identification Toolbox* from Matlab®. Both, PI and integral LQG controllers are designed for frequency locking the optical cavity using the output of the homodyne detector (error signal) as input to the controllers. Also, we present the closed-loop step response using the integral LQG controller. The error signal follows the step input without oscillations in the steady state. This is in contrast to the closed-loop step response presented in [11], [12] which showed undesired steady state oscillations in the frequency close to the first resonance in the frequency response for the plant. The closed-loop step response using the digital PI controller is also presented for comparison. The integral LQG and PI controllers are implemented using dSpace® with the Matlab® real time interface (RTI).

The rest of the paper is organized as follows: Section II discusses a block diagram for the application of digital controllers used to lock a three-mirror ring cavity to the input laser frequency. Section III describes the process of obtaining a state space model for the combined cavity and actuator system, starting with the frequency response data.

978-1-4673-4504-0/12/$31.00 ©2012 IEEE

The design process for the PI and integral LQG controllers is the subject of discussion in Section IV. A description of the experimental setup and results are outlined in Section V and the paper is concluded with final remarks in Section VI.

II. Digital Control for a Three-Mirror Optical Cavity

Fig. 1 represents a block diagram describing the implementation of digital control for a three-mirror ring cavity for cavity locking.

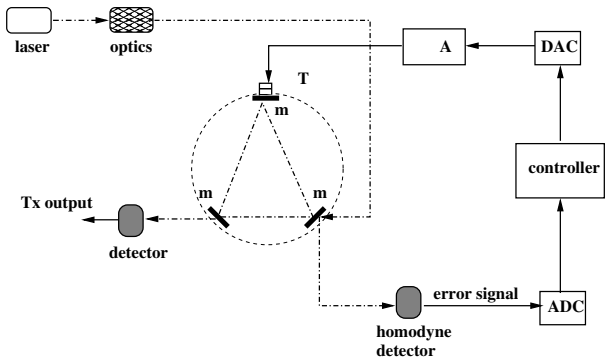

Fig. 1. Digital locking of a three-mirror ring cavity: The optical signals are represented by dash-dot lines and the electrical signals are represented as solid lines.

Light from a continuous-wave laser source is modified using optics such as isolators, mode matching optics, half wave plates, electro-optic modulators, and beam splitters, before coupling into the cavity. The cavity itself is an open-air cavity comprising of three mirrors: m1, m2, and m3. Here, a PZT is mounted on mirror m1 which is used to alter the length of the cavity. The other two mirrors m2 and m3 are rigidly fixed to the optical table. The transmitted beam (Tx output), is detected at the transmitted port by a photodetector at the output of mirror m2. The error signal is detected at mirror m3 using a homodyne detection scheme; see e.g., [11], [12]. The error signal is connected to a dSpace® analog-to-digital convertor (ADC) port which digitizes the signal to be used by the controller programmed in Matlab® RTI. The control signal is then converted back into an equivalent analog signal using a digital-to-analog converter (DAC), enhanced via a high voltage amplifier (HVA) before providing the necessary control signal to the PZT. The PZT then moves the mirror m1 based on the magnitude of the control signal applied to it.

The objective of designing a controller entails driving the error signal to zero so as to achieve cavity lock ($\Delta \approx 0$) while maintaining the transmitted signal at a maximum. This ensures that the cavity operates in a linear region as depicted in the simulated plot for the error signal in Fig. 2.

If the cavity is operating in the nonlinear region, it needs to be pushed to the linear region in order to lock the cavity. Sayed Hassen and Petersen describe a time-varying Kalman filter approach as part of an integral LQG design in [13], in simulation, to overcome this issue. This approach will

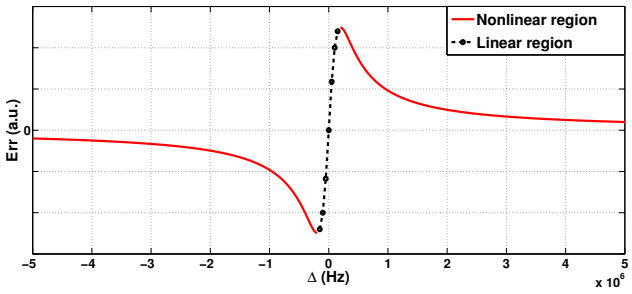

Fig. 2. Simulated variation of the error signal (output of homodyne detector) with the detuning parameter (Δ).

be considered for a later implementation and will not be discussed in this paper.

III. Cavity Model: Frequency Response and System Identification

In order to design an LQG controller to lock the cavity, we need to obtain a dynamic model for the cavity system. Though a cavity model is proposed in terms of phase and magnitude quadratures in [9], [10], [11], [12], it cannot be used directly for controller design as the model does not include the dynamics for the PZT. In order to obtain a plant model that includes the model for the cavity as well as the PZT, we record the frequency response of the plant (cavity and PZT) using a digital signal analyzer (DSA). The setup used for this purpose is shown in Fig. 3. The DSA

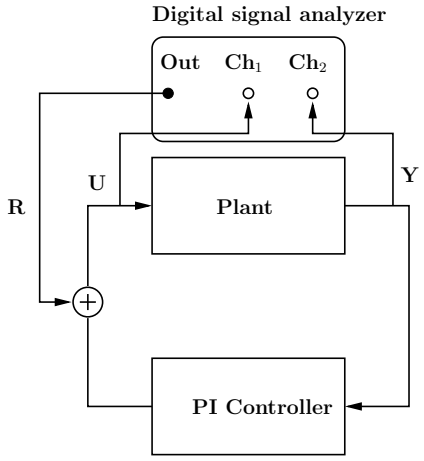

Fig. 3. Block: Digital signal analyzer setup to obtain frequency response data for the plant.

provides frequency response data in terms of the magnitude and phase of the ratio Y/U. This corresponds to the frequency response for the transfer function of the plant. During the process of data collection, the cavity was held in lock using a manually tuned analog PI controller. The corresponding frequency response is depicted in Fig. 4.

For the purpose of controller design, we consider the frequency response data up to the first resonance for the plant, which is much greater than the unity gain bandwidth of the controller. This corresponds to the magnitude information

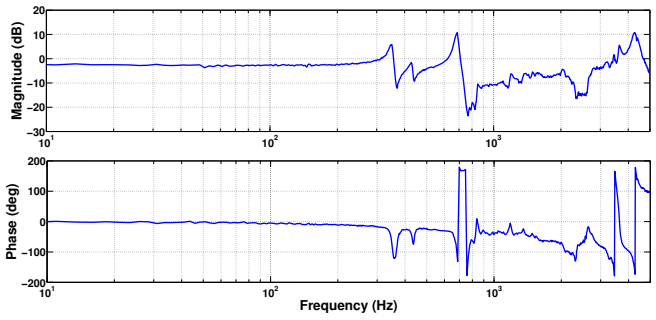

Fig. 4. Frequency response data for the plant obtained from the DSA.

in the range $0 - 400$Hz in Fig. 4, which is used to obtain a state space representation for the plant. This is achieved using the *System Identification Tool* in Matlab®. A third-order model is used to fit the desired range of data and a continuous-time state space model is obtained for the plant in the general form

$$\begin{aligned} \dot{x}(t) &= Ax(t) + Bu(t), \\ z(t) &= Cx(t) + Du(t), \end{aligned} \tag{1}$$

where

$$A = 10^4 \times \begin{bmatrix} -0.0180 & -0.2865 & 0.0573 \\ 0.1693 & -0.0157 & 0.2339 \\ 0.0446 & 0.1109 & -1.1449 \end{bmatrix};$$
$$B = \begin{bmatrix} 2.8394 \\ 4.2852 \\ -24.9287 \end{bmatrix};\ C = \begin{bmatrix} 24.0014 \\ 37.3086 \\ -34.4903 \end{bmatrix}^T;\ D = 0. \tag{2}$$

Here, $x \in \mathbb{R}^3$ is the state vector, $u \in \mathbb{R}$ is the input vector, and $z \in \mathbb{R}$ is the output.

IV. Controller Design

Two controllers were designed and digitally implemented using dSpace® and Matlab® to hold the cavity in lock. Firstly, we designed a discrete PI controller and tested its performance, followed by an integral LQG controller. These design procedures are discussed here.

A. PI Controller Design

The experimental setup in Fig. 3 used to record the frequency response data for the plant, was modified to obtain the frequency response for the analog PI controller in the feedback loop. From the magnitude plot of this data, approximate values for the proportional gain (K_P) and the integral gain (K_I) were computed according to the parallel PI controller form

$$C_{PI}(s) = K\left(K_P + \frac{K_I}{s}\right), \tag{3}$$

where K is the overall gain. Also, a low pass filter (LPF) with a cut off frequency of 600 rad/s ($\approx$ 96Hz) was added to the output of the PI controller. This inclusion of an LPF in the controller design process ensured an acceptable phase margin at the first resonance for the plant. The final transfer function ($C_{PIF}(s)$) for the overall controller was computed as a product of the transfer function for the PI controller outlined in (3) and the transfer function of the LPF as

$$C_{PIF}(s) = C_{PI}(s) * \frac{600}{s + 600}. \tag{4}$$

The transfer function in (4) was discretized with a sampling time of $30\mu s$ before implementing the controller using Matlab® RTI. The starting values used for various gains for the PI controller are outlined in Table I, which were tuned online using the ControlDesk® interface for dSpace®.

TABLE I
INITIAL GAIN VALUES USED FOR THE DESIGN OF THE DIGITAL PI CONTROLLER.

Gain constant	Value
K	30
K_P	0.05
K_I	0.08

B. LQG Integral Controller Design

As outlined in Section II, the control objective is to maintain detuning (Δ) as close to zero as possible while maximizing the transmitted signal. However, the cavity system suffers from slowly varying drifts and offsets. In order to achieve a stable cavity lock, one needs to take these effects into consideration while designing an LQG controller. One solution would be to augment an integrator with the LQG controller design as outlined in [11], [12]. We use the technique outlined in [11], [12] to design a similar integral LQG controller for implementation in this paper.

As a first step, we modify the plant output to provide two inputs to the controller as outlined in Fig. 5. The updated

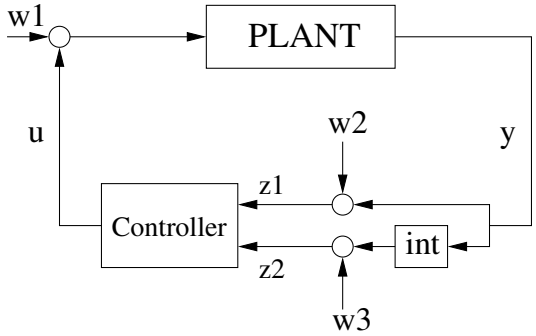

Fig. 5. Plant output augmented with an integrator.

plant model is given by

$$\dot{x}_a = A_a x_a + B_a u + B_a w_1, \tag{5}$$
$$z_a = C_a x_a + v, \tag{6}$$

where $v = [w_2\ w_3]^T$ and the augmented state and output vectors are $x_a = [x\ \int y\, dt]^T$ and $z_a = [z_1\ z_2]^T$. Also, the matrices for the augmented system are defined as

$$A_a = \begin{bmatrix} A & 0 \\ C & 0 \end{bmatrix},\ B_a = \begin{bmatrix} B \\ 0 \end{bmatrix},\ C_a = \begin{bmatrix} C & 0 \\ 0 & I \end{bmatrix}, \tag{7}$$

where x, A, B, and C are defined in (1) and (2).

For the augmented plant outlined in (5)-(7), the integral LQG controller is designed by defining a quadratic cost function of the form

$$\mathfrak{J} = \mathbb{E}\left[\frac{1}{T}\int_0^{t_f}\left(x^T Q x + f(y)^T Q_I f(y) + u^T R u\right) dt\right], \tag{8}$$

where $f(y) = \int_0^{t_f} y(\tau) d\tau$, $\mathbb{E}[\cdot]$ is the expected value, and t_f is the final time. Also, $Q \geq 0, Q_I \geq 0$, and $R > 0$ are weighting matrices associated with the state, the integral state, and the control input respectively. The integral LQG control solution is defined by the equations

$$\dot{\hat{x}}_a = A_a \hat{x}_a + B_a u + K\left(z_a - C_a \hat{x}_a\right), \tag{9}$$

$$u = -L\hat{x}_a. \tag{10}$$

Here, $\hat{x}_a$ is the augmented state vector estimated by the linear Kalman filter and K is the associated Kalman gain defined as

$$K = P_K C_a^T R_K^{-1}, \tag{11}$$

where $P_K \geq 0$ is the solution to the matrix Riccati equation

$$\dot{P}_K = A_a P_K + P_K A_a^T - P_K C_a^T R_K^{-1} C_a P_K + Q_K. \tag{12}$$

Here, $Q_K \geq 0$ and $R_K > 0$ are process and measurement noise matrices defined as

$$Q_K = \sigma_1^2, \qquad R_K = \begin{bmatrix} \sigma_2^2 & 0 \\ 0 & \sigma_3^2 \end{bmatrix}, \tag{13}$$

where σ_1 is the standard deviation associated with the process noise w_1 and represents the mechanical noise in the system. Also, σ_2 and σ_3 are the standard deviations associated with the output sensor noise (w_2) and the augmented integral output sensor noise (w_3).

The feedback gain matrix L in (10) is given by

$$L = R_C^{-1} B_a P_C, \tag{14}$$

where $P_C \geq 0$ is the solution to the matrix Riccati equation

$$\dot{P}_C = A_a P_C + P_C A_a^T - P_C C_a^T R_C^{-1} C_a P_C + Q_C \tag{15}$$

with the controller weighting matrix $R_C = r$ and

$$Q_C = C_a^T \begin{bmatrix} 1 & 0 \\ 0 & q \end{bmatrix} C_a. \tag{16}$$

Both r and q are treated as design parameters. Various parameters chosen during the design process for the integral LQG controller are outlined in Table II.

TABLE II

PARAMETER VALUES USED FOR THE DESIGN OF THE INTEGRAL LQG CONTROLLER.

Parameter	Value
σ_1^2	10^3
σ_1^2	10^3
σ_1^2	10^{-4}
r	0.5
q	10^8

The state space model for the integral LQG controller was discretized before implementing it in Matlab®. For details on LQG controller design, see e.g., [14].

A Bode plot comparing the loop-gain for the plant transfer function with the discrete integral LQG controller and the digital PI controller transfer functions is depicted in Fig. 6. Here, the gain values outlined in Table I were used to compute the loop-gain for the open-loop system with the digital PI controller, whereas, the parameter values outlined in Table II were used to compute the loop-gain for the open-loop system with the discrete integral LQG controller. A comparison of the gain margin (GM), the phase margin (PM), and the gain crossover frequency (GCF) is outlined in Table III. As seen from this comparison, the system with the discrete integral LQG controller has a greater gain crossover frequency and is hence more stable than the system with the digital PI controller that has a much smaller gain crossover frequency.

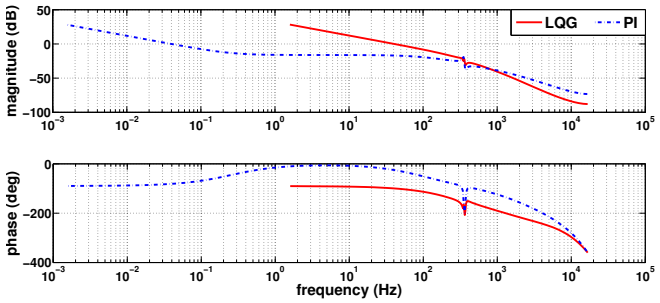

Fig. 6. Bode plot: Loop gain comparison for the plant with discrete integral LQG and digital PI controller transfer functions.

TABLE III

LOOP-GAIN: COMPARISON OF THE GAIN MARGIN (GM), THE PHASE MARGIN (PM), AND THE GAIN CROSSOVER FREQUENCY (GCF) FOR DIGITAL PI AND DISCRETE INTEGRAL LQG CONTROLLER TRANSFER FUNCTIONS WITH THE PLANT TRANSFER FUNCTION.

	GM (dB)	PM (deg)	GCF (Hz)
PI	21.2	98.9	0.04
LQG	20.8	80.3	41

V. EXPERIMENTAL SETUP AND RESULTS

Fig. 7 shows an image describing the experimental setup used to lock the three-mirror ring cavity. Fig. 8 plots the error signal and transmitted signal under integral LQG lock for this cavity. As seen from these plots, the error signal is held at zero and the transmitted signal is held constant at a maximum value of ≈ 0.73 a.u., satisfying the control objectives outlined in Section II.

In order to compare the performance of the integral LQG and digital PI controllers, the closed-loop step response was checked in terms of the plant output (error signal). Indeed, the magnitude of the input step was chosen so as to maintain cavity lock. Fig. 9 shows the setup used to check the step

Fig. 7. Experimental setup for locking the three-mirror cavity: (A) is the laser source, (B) is the triangular optical cavity, (C) is the detector at the transmitted port, and (D) is the homodyne detector.

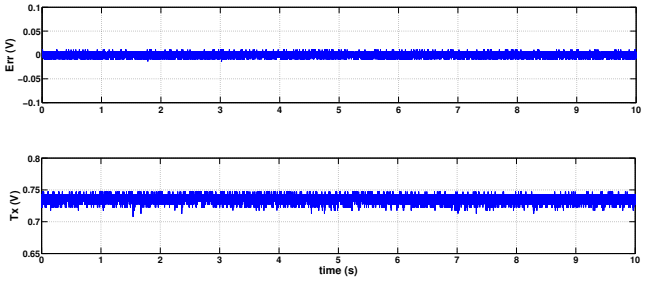

Fig. 8. Error signal and transmitted signal under integral LQG lock.

response for the closed-loop system. Fig. 10(a) plots the step response for the integral LQG controller when excited with a step input of 0.04V. The error signal which is initially at 0V, responds to this disturbance and settles within 0.1s. The zig-zag patterns in the response are due to the quantization error from the 12-bit ADC/DAC converter. However, the closed-loop step response presented in [11], [12], under integral LQG lock for a two-mirror cavity showed undesired steady-state oscillations at a frequency close to the first resonance for the plant.

As a comparison, the step response for the closed-loop system under the digital PI lock is depicted in Fig. 10(b). The

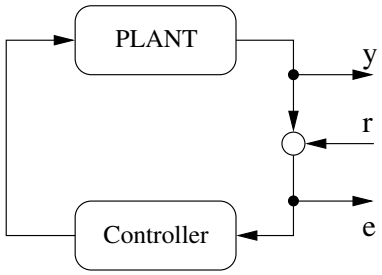

Fig. 9. Block: Setup for checking the step response of the closed-loop system.

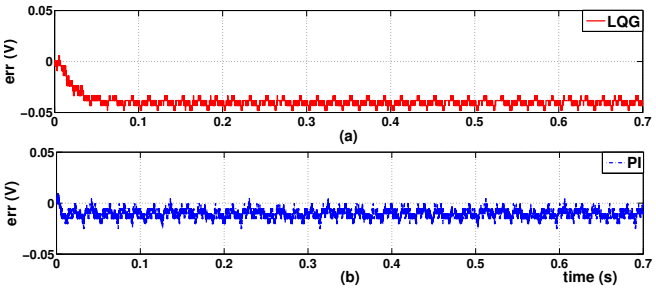

Fig. 10. Closed-loop step response under: (a) discrete integral LQG lock and (b) digital PI lock.

magnitude of the step response in this case was set to 0.015V. Though the step input is smaller than the one used for the closed-loop system with the integral LQG controller, the error signal does not settle but oscillates in the neighborhood of the steady state value for the step input. Table IV compares statistics for the steady state step response obtained using the discrete integral LQG and digital PI controllers. As seen from the comparison, the LQG controller follows the step input with better fidelity than the PI controller.

TABLE IV

COMPARISON: STEADY STATE STEP RESPONSE STATISTICS.

	r(t) (V)	mean (V)	stdev (V %)
LQG	-0.04	-0.0391	12.75
PI	-0.015	-0.0105	58

VI. CONCLUSIONS

This paper presented two methods for digitally locking a three-mirror ring cavity. Although the emphasis was on designing and implementing an integral LQG controller, a digital PI controller was also implemented in order to compare the closed-loop step response. The dynamics for the plant (cavity and piezo actuator) were obtained by recording its frequency response using a digital signal analyzer. A third-order model was fit to the frequency response data using the system identification toolbox in Matlab® and an equivalent state space model was obtained describing the dynamics for the plant. Since the first resonance for the system was recorded to be around 360Hz, which is much greater than the unity gain bandwidth for the controller, we chose a frequency window of $0 - 400$Hz for the purpose of obtaining a model for the plant. This numerically obtained plant model was then augmented with an integrator in order to design an integral LQG controller. This modification was made in order to accommodate time varying drifts and offsets in the cavity.

The integral LQG controller was programmed using Matlab® and implemented using dSpace® to lock the optical cavity. It was noted that the controller satisfied the control objectives, namely, reducing and holding the detuning parameter at zero while maximizing the transmitted signal.

In addition, results were provided for the step response of the closed-loop system and was found that the plant followed the step input with no oscillations in the steady state. This was an improvement over a previous step response presented in literature for an integral LQG lock of a two-mirror cavity that showed undesired oscillations in the steady state. As a comparison, the step response of the closed-loop system with the integral LQG controller described in this paper was compared to that obtained with a digital proportional-integral controller. It was found that the latter method demonstrated an oscillatory behavior in the steady state step response.

REFERENCES

[1] L. H. B. Dahmani and R. Drullinger, "Frequency stabilization of semiconductor lasers by resonant optical feedback," *Optics Letters*, vol. 12, no. 11, pp. 876–878, 1987.

[2] B. A. Paldus, C. C. Harb, T. G. Spence, B. Wilke, J. Xie, J. S. Harris, and R. N. Zare, "Cavity-Locked Ring-Down Spectroscopy," *Journal of Applied Physics*, vol. 83, no. 8, pp. 3991–3997, Apr. 1998.

[3] A. G. Kallapur, T. K. Boyson, I. R. Petersen, and C. C. Harb, "Nonlinear estimation of ring-down time for a fabry-perot optical cavity," *Optics Express*, vol. 19, no. 7, pp. 6377–6386, 2011.

[4] ——, "Offline estimation of ring-down time for an experimental fabry-perot optical cavity," in *IEEE International Conference on Control Applications (CCA)*, Denver, CO, USA, September 2011, pp. 556–560.

[5] H. Mabuchi and A. C. Doherty, "Cavity quantum electrodynamics: Coherence in context," *Science*, vol. 298, no. 5597, pp. 1372–1377, 2002.

[6] K. J. Vahala, "Optical microcavities," *Nature*, vol. 424, pp. 839–846, 2003.

[7] F. V. Jan Klaers, Julian Schmitt and M. Weitz, "Bose-Einstein Condensation of Photons in an Optical Microcavity," *Nature*, vol. 468, pp. 545–548, 2010.

[8] J. Ye and T. W. Lynn, "Applications of optical cavities in modern atomic, molecular, and optical physics," ser. Advances In Atomic, Molecular, and Optical Physics. Academic Press, 2003, vol. 49, pp. 1–83.

[9] E. H. Huntington, M. R. James, and I. R. Petersen, "Modern quantum control applied to optical cavity locking," in *Australian Institute of Physics 17th National Congress 2006*, Brisbane, QLD, December 2006.

[10] ——, "Laser-cavity frequency locking using modern control," in *46th IEEE Conference on Decision and Control*, New Orleans, LA, USA, December 2007, pp. 6346 – 6351.

[11] S. Z. Sayed Hassen, E. H. Huntington, I. R. Petersen, and M. R. James, "Frequency locking of an optical cavity using LQG integral control," in *Proceedings of the 17th IFAC World Congress*, Seoul, Korea, July 2008, pp. 1821–1826.

[12] S. Z. S. Hassen, M. Heurs, E. H. Huntington, I. R. Petersen, and M. R. James, "Frequency locking of an optical cavity using linear quadratic Gaussian integral control," *Journal of Physics B: Atomic, Molecular and Optical Physics*, vol. 42, p. 175501, 2009.

[13] S. Z. Sayed Hassen and I. R. Petersen, "A time-varying Kalman filter approach to integral LQG frequency locking of an optical cavity," in *American Control Conference*, Baltimore, MD, USA, June 2010, pp. 2736–2741.

[14] D. E. Kirk, *Optimal Control Theory: An Introduction*. Mineola, NY, USA: Dover Publications, 1998.